

SC-KF Mobile Robot Localization: A Stochastic Cloning-Kalman Filter for Processing Relative-State Measurements

Anastasios I. Mourikis[†], Stergios I. Roumeliotis[†], and Joel W. Burdick[‡]

Abstract—This paper presents a new method to optimally combine *motion* measurements provided by proprioceptive sensors, with *relative-state* estimates inferred from feature-based matching. Two key challenges arise in such *pose tracking* problems: (i) the displacement estimates relate the state of the robot at *two* different time instants, and (ii) the same exteroceptive measurements are often used for computing consecutive displacement estimates, a process which leads to correlations in the errors. We present a novel *Stochastic Cloning-Kalman Filtering* (SC-KF) estimation algorithm that successfully addresses these challenges, while still allowing for efficient calculations of the filter gains and covariances. The proposed algorithm is not intended to compete with Simultaneous Localization and Mapping (SLAM) approaches. Instead it can be merged with any EKF-based SLAM algorithm to increase its precision. In this respect, the SC-KF provides a robust framework for leveraging additional motion information extracted from dense point features that most SLAM algorithms do not treat as landmarks. Extensive experimental and simulation results are presented to verify the validity of the method and to demonstrate that its performance is superior to that of alternative position tracking approaches.

Index Terms—Stochastic Cloning, robot localization, relative-pose measurements, displacement estimates, state augmentation.

I. INTRODUCTION

Accurate localization is a prerequisite for a robot to meaningfully interact with its environment. The most commonly available sensors for acquiring localization information are *proprioceptive* sensors, such as wheel encoders, gyroscopes, and accelerometers, that provide information about the robot's motion. In Dead Reckoning (DR) [1], a robot's pose can be tracked from a starting point by integrating proprioceptive measurements over time. The limitation of DR is, however, that since no external reference signals are employed for correction, estimation errors accumulate over time, and the pose estimates drift from their real values. In order to improve *localizaton accuracy*, most algorithms fuse the proprioceptive measurements with data from *exteroceptive* sensors, such as cameras [2], [3], laser range finders [4] sonars [5], etc.

When an exteroceptive sensor provides information about the position of features with respect to the robot at two different time instants, it is possible (under necessary observability assumptions) to create an *inferred* measurement of the robot's *displacement*. Examples of algorithms that use exteroceptive data to infer motion include laser scan matching [4], [6], [7], vision-based motion estimation techniques using stereoscopic [2], [3], and monocular [8] image sequences, and

[†]Dept. of Computer Science & Engineering, University of Minnesota, Minneapolis, MN 55455. Email: {mourikis|stergios}@cs.umn.edu. [‡]Division of Engineering and Applied Science, California Institute of Technology, Pasadena, CA 91125. Email: jwb@robotics.caltech.edu.

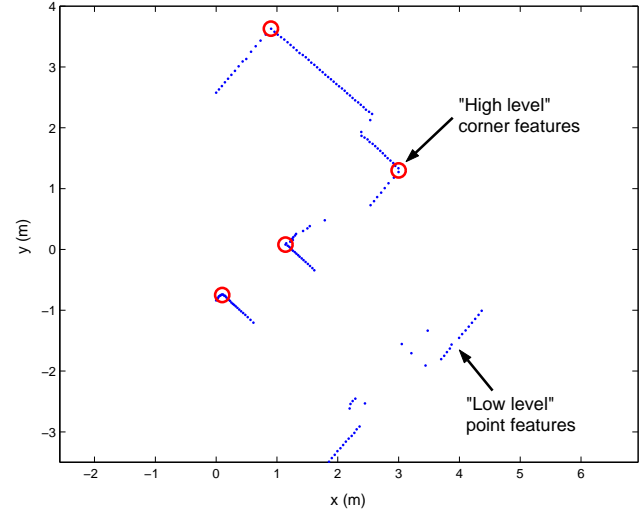


Fig. 1. Example of a planar laser scan and types of features observed. An algorithm has been employed to detect corners (intersections of line segments) in a laser scan. The extracted corner features can be used for performing SLAM, while all the remaining, “low-level”, feature points, can be utilized in the SC-KF framework to improve the pose tracking accuracy.

matching of sonar returns [5]. The inferred *relative-state* measurements that are derived from these measurements can be integrated over time to provide pose estimates [3], or combined with proprioceptive sensory input in order to benefit from both available sources of positioning information [9], [10]. This paper focuses on how to optimally implement the latter approach using an Extended Kalman Filter (EKF) [11]. This paper does not consider the case in which the feature measurements are used for SLAM. However, as discussed in Section VI, our approach is complementary to SLAM, and can be employed to increase its accuracy (cf. Fig. 1).

Two challenges arise when fusing relative-pose¹ measurements with proprioceptive measurements within an EKF. Firstly, each displacement measurement relates the robot's state at two *different* time instants (i.e., the current time and previous time when exteroceptive measurements were recorded). However, the basic theory underlying the EKF requires that the measurements used for the state update be *independent* of any previous filter states. Thus, the “standard” formulation of the EKF, in which the filter's state comprises only the *current* state of the robot, is clearly not adequate for

¹Throughout this paper, the terms “displacement measurement” and “relative-pose measurement” are used interchangeably to describe a measurement of the robot's motion that is inferred from exteroceptive measurements. Depending on the type and number of available features, either all, or a subset, of the degrees of freedom of motion may be determined (cf. Section VII-A.2).

treating relative-state measurements.

A second challenge arises from the fact that when exteroceptive measurements are used to infer displacement, consecutive relative-state measurements will often be *correlated*. To understand the source of such correlations, consider, for example, the scenario in which a camera is employed to measure the pixel coordinates of the projections of the same landmarks at time-steps $k - 1$, k and $k + 1$. The errors in the measurements at time step k affect the displacement estimates for both time intervals $[k - 1, k]$ and $[k, k + 1]$, thereby rendering them correlated. However, assuming that the measurements are uncorrelated (as is customarily done [2], [7], [10]), violates a basic assumption of EKF theory, leading to sub-optimal or incorrect estimates for the robot's state and covariance. This fact has been generally overlooked in the literature, and to the best of our knowledge, no prior work exists that directly addresses this issue.

In this paper we propose a direct approach to the problem of combining relative-pose measurements with proprioceptive measurements in order to improve the accuracy of DR. Our methodology *augments* the state vector of the Kalman filter in order to address the two aforementioned challenges. In particular, to properly account for the dependencies of the robot's state estimates at different time instants, we augment the the Kalman filter state to include two instances (or "clones") of the state estimate—hence the name *Stochastic Cloning Kalman Filter (SC-KF)* [9]. Moreover, in order to appropriately treat the correlations between consecutive displacement estimates, we further augment the state to include the most recent *exteroceptive measurements* [12]. As described in Section III, with these state augmentations the displacement measurements can be expressed as functions of the *current filter state*, and thus an EKF framework can be employed.

The following section reviews existing approaches for processing relative-state measurements, while Section III describes our new approach. Section IV develops the propagation of the state covariance in the important special case where *only* displacement measurements are used for localization. Section V presents extensions of the SC-KF methodology, while Section VI describes its relation to SLAM. In Section VII, it is shown that the attained position tracking accuracy is superior to that of existing approaches. Finally, the conclusions of this work are presented in Section VIII.

II. RELATED APPROACHES

Displacement measurements can be treated as *average velocity measurements* during the corresponding time-interval. These *average velocities* can then be combined with velocity measurements obtained from the robot's proprioceptive sensors to improve their accuracy. However, this approach is only applicable if the relative-state measurements are made at a rate equal or higher to that of the proprioceptive sensors, which is rarely the case in practice. Alternatively, the robot's velocity estimate could be included in the state vector, and the average velocity estimates could then be used as instantaneous velocity pseudo-measurements in the EKF update step [13]. The shortcoming of this method is that treating an *average* velocity measurement as an *instantaneous* one can introduce

significant errors when the rate of the displacement measurements is low. A different solution, proposed in [10], is to use the previous robot position estimates for converting the relative pose measurements to *absolute position pseudo-measurements*. However, since these pseudo-absolute measurements are correlated with the state, their covariance matrix has to be artificially inflated to guarantee consistency, thus resulting in suboptimal estimation (cf. Section VII-A).

Contrary to the preceding *ad-hoc* methods for processing displacement measurements, several existing approaches employ these measurements to *provide* constraints between consecutive robot poses. Algorithms that *only* use displacement measurements for propagating the robot's state estimate are often described as sensor-based odometry methods [2], [4]. In these algorithms, only the last two robot poses (the current and previous one) are ever considered. While our stochastic cloning approach (which was first introduced in [9]) also relies only upon the last two robot poses, tracking is achieved by *optimally fusing* the displacement measurements with proprioceptive information. Therefore, our method can be seen as an "enhanced" form of odometry. On the other hand, several existing approaches maintain a state vector comprised of a *history* of robot poses, and use the displacement measurements to impose constraints between pairs of these poses. In [14], the robot's orientation errors are assumed to be temporally uncorrelated, which transforms the problem of optimizing the network of robot poses into a linear one, where only the robot positions are estimated. In [15]–[17] the full 3D robot pose of an autonomous underwater vehicle is estimated, while in [7], [18] displacement constraints are employed for estimating the pose history of a robot in 2D.

All of the approaches discussed so far do not properly account for the correlations that exist between consecutive displacement estimates, as they are assumed to be *independent*. However, as shown in Section III-A, this assumption does *not* generally hold. One could avoid such correlations by using each feature measurement in the computation of *one* displacement estimate [15]. For example, half the measurements at each time step can be used to estimate the previous displacement, and the other half to estimate the next one. The drawback of this methodology is that *incorporating* only *part* of the available exteroceptive measurements when computing each relative pose estimate results in less accurate displacement estimates. In our work, *all* available measurements are used to compute the relative-pose measurements at every time-step, and the correlations that are introduced by this process are explicitly identified and accounted for.

Solutions to the well-known Simultaneous Localization and Mapping (SLAM) problem (cf. Section VI). "circumvent" the problem of treating the displacement measurements by including the *features'* positions in the state vector, and jointly estimating the robot's and features' state. While SLAM offers high localization accuracy, the computational complexity associated with the estimation of the positions of a large number of features results may be prohibitive for some real time applications (e.g., autonomous aircraft landing). Thus there exists a need for methods that enable *direct* processing of the displacement measurements, at a lower computational cost.

In this paper, we propose an algorithm for optimally fusing the potentially correlated relative displacement estimates with proprioceptive measurements. In this algorithm, the exteroceptive measurements are considered in pairs of consecutive measurements, that are first processed in order to create an inferred *relative-pose* measurement, and then fused with the proprioceptive measurements. The sole objective of the algorithm is to estimate the robot's state, and therefore the states of features that are employed for deriving the displacement measurements are not estimated. Hence the proposed algorithm can optimally fuse relative-pose measurements with the minimum computational overhead (Section III-F). The proposed method can be used either as a stand-alone localization algorithm, or combined with SLAM in order to increase its localization accuracy (cf. Section VI).

III. FILTERING WITH CORRELATED RELATIVE-STATE MEASUREMENTS

A. Relative-pose Measurement Correlations

Before presenting the Stochastic Cloning Kalman Filter (SC-KF), we first study the structure of the correlations between consecutive displacement estimates. Let z_k and z_{k+m} denote the vectors of exteroceptive measurements at time-steps k and $k+m$, respectively, whose covariance matrices are R_k and R_{k+m} . These are measurements, for example, of range and bearing from a laser range finder, or of bearing from a camera. By processing these measurements (e.g., via laser scan matching), an estimate, $z_{k/k+m}$, for the change in the robot pose between time-steps k and $k+m$ is computed as a function (either closed-form or implicit) of z_k and z_{k+m} :

$$z_{k/k+m} = \xi_{k/k+m}(z_k, z_{k+m}) \quad (1)$$

The linearization of (1) relates error in the displacement estimate, $\tilde{z}_{k/k+m}$, to errors in the exteroceptive measurements:²

$$\tilde{z}_{k/k+m} \simeq J_{k/k+m}^k \tilde{z}_k + J_{k/k+m}^{k+m} \tilde{z}_{k+m} + n_{k/k+m} \quad (2)$$

where the noise term $n_{k/k+m}$ arises from inaccuracies in the displacement estimation algorithm (e.g., errors due to feature matching [6]). We assume that the exteroceptive measurement errors, \tilde{z}_k and \tilde{z}_{k+m} , and the noise term, $n_{k/k+m}$, are zero-mean and independent, an assumption which holds in most practical cases if proper sensor characterization is performed. In (2), $J_{k/k+m}^k$ and $J_{k/k+m}^{k+m}$ are the Jacobians of the function $\xi_{k/k+m}$ with respect to z_k and z_{k+m} , respectively, i.e.,

$$J_{k/k+m}^k = \nabla_{z_k} \xi_{k/k+m} \quad \text{and} \quad J_{k/k+m}^{k+m} = \nabla_{z_{k+m}} \xi_{k/k+m}$$

The indices in the vector $z_k^T = [z_{k_1}^T \dots z_{k_{M_k}}^T]$ are bizarre. It should really be something like $z_k^T = [(z_k)_1^T \dots (z_k)_M^T]$

²The “hat” symbol, $\hat{\cdot}$, is used to denote the estimated value of a quantity, while the “tilde” symbol, $\tilde{\cdot}$, is used to signify the error between the actual value of a quantity and its estimate. The relationship between a variable, x , its estimate, \hat{x} , and the error \tilde{x} , is $\tilde{x} = x - \hat{x}$.

Generally, not all feature measurements in the vector z_k are used to estimate displacement. For example, in laser scan matching there usually exists only partial overlap between consecutive scans and therefore not all laser returns are matched. As a result, if M_k denotes the number of feature measurements in $z_k^T = [z_{k_1}^T \dots z_{k_{M_k}}^T]$, the *i*th component of the Jacobian matrices $J_{k/k+m}^k$ and $J_{k/k+m}^{k+m}$ will take the form

$$(J_{k/k+m}^t)_i = \begin{cases} \nabla_{z_{t_i}} \xi_{k/k+m}, & \text{i} \text{th feature used} \\ & \text{to compute } z_{k/k+m} \\ 0, & \text{else} \end{cases} \quad (3)$$

for $i = 1 \dots M_k$ and $t \in \{k, k+m\}$. Thus for some applications, the Jacobians may be significantly sparse.

Our goal is to compute the correlation between the displacement estimates for the time intervals $[k-\ell, k]$ and $[k, k+m]$, which is defined as $E\{\tilde{z}_{k-\ell/k} \tilde{z}_{k/k+m}^T\}$. For this purpose we employ (2), and the independence of exteroceptive measurement errors at different time-steps, to obtain:

$$\begin{aligned} E\{\tilde{z}_{k-\ell/k} \tilde{z}_{k/k+m}^T\} &= J_{k-\ell/k}^k E\{\tilde{z}_k \tilde{z}_k^T\} J_{k/k+m}^{k T} \\ &= J_{k-\ell/k}^k R_k J_{k/k+m}^{k T} \end{aligned} \quad (4)$$

Note that exteroceptive measurements typically consist of a relatively small number of features detected in the robot's vicinity (e.g., distance and bearing to points on a wall, or the image coordinates of visual features). In such cases, the measurements of the individual features are mutually independent, and therefore the covariance matrix R_k is block diagonal. In light of (3), when R_k is block diagonal, expression (4) is if different features are used to estimate displacement in consecutive time intervals (i.e., if non-overlapping subsets of z_k are matched with $z_{k-\ell}$ and z_{k+m} , respectively). Clearly, this is not the case in general, and thus consecutive displacement estimates are in most cases not independent.

B. EKF Formulation

We now describe the formulation of an Extended Kalman filter (EKF) estimator that can fuse proprioceptive and relative-pose measurements, while properly accounting for the correlations in the latter.

To reiterate the challenge posed in Section I, displacement measurements relate two robot states, and therefore the joint pdf of these states must be available in the filter. For this reason, we augment the EKF (error) state vector³ to include two copies of the robot's error state (cloning) [9]. The first copy of the error vector, \tilde{X}_k , represents the pose error at the instant when the latest exteroceptive measurement was recorded, while the second copy, \tilde{X}_{k+i} , represents the error in the robot's current state. In the propagation phase of the filter, only the current (evolving) state is propagated, while the previous state remains unchanged. Consequently, the robot states related by each displacement estimate are both represented explicitly in the filter state.

³Since the extended form of the Kalman filter is employed for estimation, the state vector comprises the errors in the estimated quantities, rather than the estimates. Therefore, cloning has to be applied to both the error states, and the state estimates.

To correctly account for the correlations between consecutive relative-state measurements, the state vector is additionally augmented to include the *measurement errors* of the latest exteroceptive measurement [12]. Thus, if the most recent exteroceptive measurement was recorded at t_k , the filter's error-state vector at t_{k+i} is:

$$\check{X}_{k+i|k} = \begin{bmatrix} \tilde{X}_{k|k}^T & \tilde{X}_{k+i|k}^T & \tilde{z}_k^T \end{bmatrix}^T \quad (5)$$

where the subscript $\ell|j$ denotes the value of a quantity at time step ℓ , after exteroceptive measurements up to time-step j , and proprioceptive measurements up to time-step $\ell-1$, have been processed. By including the measurement error in the **system's state vector**, the dependency of the relative-state measurement z_{k+k+i} on the exteroceptive measurement z_k is transformed into a dependency on the *current state of the filter*, and the problem can now be treated in the standard EKF framework. It should be noted that since the measurement error is the source of the correlation between the current and previous displacement estimates, it is the "minimum-length" vector that must be appended to the state vector in order to incorporate the existing dependencies. Thus, as explained in Section III-F, this approach yields the minimal computational overhead needed to account for these correlation.

C. Filter Initialization

Consider the case where the first exteroceptive measurement, z_0 , is taken at time $t_0 = 0$ and let the robot's corresponding state estimate and covariance be denoted by $\hat{X}_{0|0}$ and $P_{0|0}$, respectively. The initial error-state vector for the SC-KF contains the robot state and its clone, as well as the errors of the exteroceptive measurements at time step 0 (cf. (5)):

$$\check{X}_{0|0} = \begin{bmatrix} \tilde{X}_{0|0}^s & \tilde{X}_{0|0}^T & \tilde{z}_0^T \end{bmatrix}^T \quad (6)$$

The superscript s in (6) refers to the static copy of the state, which will remain unchanged during propagation.

Cloning of the robot state creates two identical random variables that convey the same information, and are thus fully correlated. Moreover, since the exteroceptive measurement at t_0 is not used to estimate the initial robot state, the latter is independent of the error \tilde{z}_0 . Thus, the initial covariance matrix of the SC-KF state vector has the form:

$$\check{P}_{0|0} = \begin{bmatrix} P_{0|0} & P_{0|0} & 0 \\ P_{0|0} & P_{0|0} & 0 \\ 0 & 0 & R_0 \end{bmatrix}. \quad (7)$$

D. State Propagation

During normal operation, the filter's state covariance matrix, immediately after the relative-state measurement $z_{k-\ell/k} = \xi_{k-\ell/k}(z_{k-\ell}, z_k)$ has been processed, takes the form:

$$\check{P}_{k|k} = \begin{bmatrix} P_{k|k} & P_{k|k} & P_{X_k z_k} \\ P_{k|k} & P_{k|k} & P_{X_k z_k} \\ P_{X_k z_k}^T & P_{X_k z_k}^T & R_k \end{bmatrix} \quad (8)$$

where $P_{k|k}$ is the covariance of the robot state at t_k , R_k is the covariance matrix of the error \tilde{z}_k , and $P_{X_k z_k} = E\{\tilde{X}_k \tilde{z}_k^T\}$

is the cross-correlation between the robot's state and the measurement error at t_k (a closed-form expression for $P_{X_k z_k}$ is derived in Section III-E). Between two consecutive updates, proprioceptive measurements are employed to propagate the filter's state and its covariance. The robot's state estimate is propagated in time by the, generally non-linear, equation:

$$\hat{X}_{k+1|k} = f(\hat{X}_{k|k}, v_k) \quad (9)$$

where v_k denotes the proprioceptive (e.g., linear and rotational velocity) measurement at t_k . Linearization of (9) yields the error-propagation equation for the (evolving) second copy of the robot state:

$$\check{X}_{k+1|k} \simeq F_k \hat{X}_{k|k} + G_k \tilde{v}_k \quad (10)$$

where F_k and G_k are the Jacobians of $f(\hat{X}_{k+1|k}, v_k)$ with respect to $\hat{X}_{k|k}$ and v_k , respectively. Since the cloned state, $X_{k|k}^s$, as well as the estimates for the measurement error \tilde{z}_k , do not change with the integration of a new proprioceptive measurement (i.e., $X_{k+1|k}^s = X_{k|k}^s$), the error propagation equation for the augmented state vector is:

$$\check{X}_{k+1|k} = \check{F}_k \check{X}_{k|k} + \check{G}_k \tilde{v}_k \quad (11)$$

$$\text{with } \check{F}_k = \begin{bmatrix} I & 0 & 0 \\ 0 & F_k & 0 \\ 0 & 0 & I \end{bmatrix} \quad \text{and} \quad \check{G}_k = \begin{bmatrix} 0 \\ G_k \\ 0 \end{bmatrix} \quad (12)$$

. Thus the covariance matrix of the propagated filter state is:

$$\check{P}_{k+1|k} = \check{F}_k \check{P}_{k|k} \check{F}_k^T + \check{G}_k Q_k \check{G}_k^T = \begin{bmatrix} P_{k|k} & P_{k|k} F_k^T & P_{X_k z_k} \\ F_k P_{k|k} & F_k P_{k|k} F_k^T + G_k Q_k G_k^T & F_k P_{X_k z_k} \\ P_{X_k z_k}^T & P_{X_k z_k}^T F_k^T & R_k \end{bmatrix} \quad (13)$$

where $Q_k = E\{\tilde{v}_k \tilde{v}_k^T\}$ is the covariance of the proprioceptive measurement v_k .

By straightforward calculation, if m propagation steps occur between two consecutive relative-state updates, the covariance matrix $\check{P}_{k+m|k}$ is determined as

$$\check{P}_{k+m|k} = \begin{bmatrix} P_{k|k} & P_{k|k} \mathcal{F}_{k+m|k}^T & P_{X_k z_k} \\ \mathcal{F}_{k+m|k} P_{k|k} & P_{k+m|k} & \mathcal{F}_{k+m|k} P_{X_k z_k} \\ P_{X_k z_k}^T \mathcal{F}_{k+m|k}^T & P_{X_k z_k}^T & R_k \end{bmatrix} \quad (14)$$

where $\mathcal{F}_{k+m|k} = \prod_{i=0}^{m-1} F_{k+i}$, and $P_{k+m|k}$ is the propagated covariance of the robot state at t_{k+m} . The form of (14) shows that the covariance matrix of the filter can be propagated with minimal computation. In an implementation where efficiency is of utmost importance, the product $\mathcal{F}_{k+m|k}$ can be accumulated, and the matrix multiplications necessary to compute $\check{P}_{k+m|k}$ can be delayed and carried out only when a new exteroceptive measurement is processed.

E. State Update

We next consider the state update step of the SC-KF filter. Assume that a new exteroceptive measurement, z_{k+m} , is recorded at t_{k+m} , and along with z_k it is used to produce a relative-state measurement, $z_{k/k+m} = \xi_{k/k+m}(z_k, z_{k+m})$, relating robot poses X_k and X_{k+m} . Note that $z_{k/k+m}$ may not

fully determine all the degrees of freedom of the pose change between t_k and t_{k+m} . For example, the scale is unobservable when using a single camera to estimate displacement via point-feature correspondances [8]. Thus, the relative-state measurement is equal to a nonlinear function of the robot poses at t_k and t_{k+m} , with the addition of error:

$$z_{k/k+m} = h(X_k, X_{k+m}) + \tilde{z}_{k/k+m} . \quad (15)$$

The expected value of $z_{k/k+m}$ is computed from the state estimates at t_k and t_{k+m} , as

$$\hat{z}_{k/k+m} = h(\hat{X}_{k|k}, \hat{X}_{k+m|k}) \quad (16)$$

and therefore, based on (2), the innovation is given by:

$$r_{k+m} = z_{k/k+m} - \hat{z}_{k/k+m} \quad (17)$$

$$\begin{aligned} &\simeq \begin{bmatrix} H_k & H_{k+m} & J_{k/k+m}^k \end{bmatrix} \begin{bmatrix} \tilde{X}_{k|k} \\ \tilde{X}_{k+m|k} \\ \tilde{z}_k \end{bmatrix} \\ &+ \begin{bmatrix} J_{k/k+m}^{k+m} & I \end{bmatrix} \begin{bmatrix} \tilde{z}_{k+m} \\ n_{k/k+m} \end{bmatrix} \\ &= \check{H}_{k+m} \check{X}_{k+m|k} + \check{\Xi}_{k+m} \check{w}_{k+m} \end{aligned} \quad (18)$$

where H_k and H_{k+m} are the Jacobians of $h(X_k, X_{k+m})$ with respect to X_k and X_{k+m} , respectively.

Equation (18) demonstrates that if previous exteroceptive measurement errors, \tilde{z}_k , are incorporated in the state vector, the innovation of each measurement can be expressed as the sum of an error term dependent on the augmented state and a noise term that is independent of the state and *temporally uncorrelated*. Thus, using this approach the Kalman filter equations can now be applied to the augmented system to update the state. The residual covariance is equal to

$$\check{S} = \check{H}_{k+m} \check{P}_{k+m|k} \check{H}_{k+m}^T + J_{k/k+m}^{k+m} R_{k+m} J_{k/k+m}^{k+m T} + R_{n_{k/k+m}} \quad (19)$$

where $R_{n_{k/k+m}}$ is the covariance of the noise term $n_{k/k+m}$. The Kalman gain is computed as:

$$\check{K} = \check{P}_{k+m|k} \check{H}_{k+m}^T \check{S}^{-1} = [K_k^T \quad K_{k+m}^T \quad K_{z_k}^T]^T \quad (20)$$

We note that although the measurement z_{k+m} can be used to update the estimates of the robot's pose at t_k and for the measurement error \tilde{z}_k , our goal is to update only the current robot state at t_{k+m} and its covariance. Therefore, only the corresponding block element K_{k+m} of the Kalman gain matrix need be computed. Its formula is:

$$\begin{aligned} K_{k+m} &= (\mathcal{F}_{k+m/k} P_{k|k} H_k^T + P_{k+m|k} H_{k+m}^T \\ &+ \mathcal{F}_{k+m/k} P_{X_k z_k} J_{k/k+m}^k)^T \check{S}^{-1} . \end{aligned} \quad (21)$$

Using this result, the equations for updating the *current* robot state and covariance are:

$$\hat{X}_{k+m|k+m} = \hat{X}_{k+m|k} + K_{k+m} r_{k+m} \quad (22)$$

$$P_{k+m|k+m} = P_{k+m|k} - K_{k+m} \check{S} K_{k+m}^T . \quad (23)$$

The state update process is completed by computing the augmented covariance matrix, which is required to process the next relative-state measurement. After $z_{k/k+m}$ is processed,

Algorithm 1 Stochastic Cloning Kalman filter

Initialization: When the first exteroceptive measurement is received:

- clone the state estimate $\hat{X}_{0|0}$
- initialize the filter state covariance matrix using (7)

Propagation: For each proprioceptive measurement:

- propagate the evolving copy of the robot state via (9)
- propagate the filter covariance using (13), or equivalently (14)

Update: For each exteroceptive measurement:

- compute the relative-state measurement using (1), and its Jacobians with respect to the current and previous exteroceptive measurement, using (3).
 - update the current robot state using equations (16), (17), (19), (21), and (22)
 - update the robot state covariance matrix using (23)
 - remove the previous robot state and exteroceptive measurement
 - create a cloned copy of the current robot state
 - compute the covariance of the new augmented state vector (cf. (24)) using (26) and (27)
-

the clone of the previous state error, $\tilde{X}_{k|k}$, and the previous measurement error, \tilde{z}_k , are discarded. The robot's current state, $X_{k+m|k+m}$, is cloned, and the exteroceptive measurement errors, \tilde{z}_{k+m} , are appended to the new filter state. Thus, the filter error-state vector becomes

$$\check{X}_{k+m|k+m} = [\tilde{X}_{k+m|k+m}^T \quad \tilde{X}_{k+m|k+m}^T \quad \tilde{z}_{k+m}^T]^T \quad (24)$$

To compute the new filter covariance matrix $\check{P}_{k+m|k+m}$, the correlation between the robot's error-state estimate, $\tilde{X}_{k+m|k+m}$, and the measurement error vector, \tilde{z}_{k+m} , must be determined. From (22) we obtain:

$$\tilde{X}_{k+m|k+m} = \hat{X}_{k+m|k} - K_{k+m} r_{k+m} . \quad (25)$$

Substitution from (18) yields:

$$\begin{aligned} P_{X_{k+m} z_{k+m}} &= E\{\tilde{X}_{k+m|k+m} \tilde{z}_{k+m}^T\} \\ &= E\{\tilde{X}_{k+m|k} \tilde{z}_{k+m}^T\} - K_{k+m} E\{r_{k+m} \tilde{z}_{k+m}^T\} \\ &= -K_{k+m} E\{r_{k+m} \tilde{z}_{k+m}^T\} \\ &= -K_{k+m} J_{k/k+m}^{k+m} R_{k+m} , \end{aligned} \quad (26)$$

where the statistical independence of the error \tilde{z}_{k+m} to the errors in the propagated state $\hat{X}_{k+m|k}$ has been employed in this derivation. Based on this result, the covariance matrix of the augmented state at t_{k+m} , after the update has been performed, can be expressed as:

$$\check{P}_{k+m|k+m} = \begin{bmatrix} P_{k+m|k+m} & P_{k+m|k+m} & P_{X_{k+m} z_{k+m}} \\ P_{k+m|k+m} & P_{k+m|k+m} & P_{X_{k+m} z_{k+m}} \\ P_{X_{k+m} z_{k+m}}^T & P_{X_{k+m} z_{k+m}}^T & R_{k+m} \end{bmatrix} \quad (27)$$

For clarity, the steps of the SC-KF algorithm are outlined in Algorithm 1.

F. Computational Complexity

While our proposed state augmentation approach does correct for the correlations that have been neglected in previous work, its use imposes a cost in terms of computation and memory requirements. We now show that these algorithmic requirements are *linear* in the number of features observed at a single time-step.

If N and M_k respectively denote the dimensions of the robot's state and the size of the *measurement vector* at t_k , then the covariance matrix $\check{P}_{k+m|k}$ has size $(2N + M_k) \times (2N + M_k)$. If $M_k \gg N$, the overhead of state augmentation is mostly due to the inclusion of the measurements in the filter state vector, which leads to a correct treatment of the temporal correlations in the relative-pose measurements. If these correlations are ignored, the size of the filter state vector is twice the size of the robot's state vector. In this case, the computational complexity and memory requirements are $\mathcal{O}(N^2)$. In the algorithm proposed in this paper, the most computationally expensive operation, for $M_k \gg N$, is the evaluation of the covariance of the residual (cf. (19)). The covariance matrix $\check{P}_{k+m|k}$ is of dimensions $(2N + M_k) \times (2N + M_k)$, and thus the computational complexity of obtaining \check{S} is generally $\mathcal{O}((2N + M_k)^2) \approx \mathcal{O}(N^2 + M_k^2)$. However, as explained in Section III-A, the measurement noise covariance matrices R_k and R_{k+m} are commonly block diagonal. By exploiting the structure of $\check{P}_{k+m|k}$, the computational complexity of evaluating (19) reduces to $\mathcal{O}(N^2 + M_k)$. Moreover, when the matrices R_k and R_{k+m} are block diagonal, the covariance matrix $\check{P}_{k+m|k}$ is sparse, which reduces the storage requirements of the algorithm to $\mathcal{O}(N^2 + M_k)$ as well.

For a number of applications, it is *not* necessary to maintain a clone of the entire robot state and its covariance. Close inspection of the filter update equations reveals that only the states that *directly affect* the relative-state measurement (i.e., those that are needed to compute the expected relative-state measurement $z_{k/k+m}$ and its Jacobian, \check{H}_{k+m}) are required for the update step. The remaining states and their covariance need not be cloned, thus further reducing the memory and computational requirements. For example, when measurements from an inertial measurement unit (IMU) are employed for localization, estimates for the bias of the IMU measurements are often included in the state vector [19]. These bias estimates clearly do not appear in (16), and therefore it is not necessary to maintain their clones in the filter.

IV. STATE PROPAGATION BASED EXCLUSIVELY ON DISPLACEMENT ESTIMATES

The preceding section presented the SC-KF algorithm in the general case when both relative-state measurements and proprioceptive measurements are available for fusion. In many cases, however, no reliable proprioceptive information is available and displacement measurements *only* must be used to propagate the estimate of the robot's pose (e.g., [2], [4]). This section adapts the analysis of Section III-A to these cases, while still properly accounting for the correlations between consecutive displacement estimates.

Once the displacement estimate between time-steps k and $k+1$ has been computed (cf. (1)), an estimate for the robot's

pose at t_{k+1} is realized by combining the previous pose estimate and the displacement measurement:

$$\hat{X}_{k+1} = g(\hat{X}_k, z_{k/k+1}). \quad (28)$$

By linearizing this equation, the pose errors at t_{k+1} can be related to the errors in the previous state estimate and displacement measurement:

$$\tilde{X}_{k+1} \simeq \Phi_k \tilde{X}_k + \Gamma_k \tilde{z}_{k/k+1} \quad (29)$$

where Φ_k and Γ_k represent the Jacobians of the state propagation function, $g(\hat{X}_k, z_{k/k+1})$, with respect to the previous pose and the relative pose measurement, respectively:

$$\Phi_k = \nabla_{\hat{X}_k} g, \quad \Gamma_k = \nabla_{\tilde{z}_{k/k+1}} g. \quad (30)$$

The covariance matrix of the pose estimates is propagated by:

$$\begin{aligned} P_{k+1} &= E\{\tilde{X}_{k+1} \tilde{X}_{k+1}^T\} \\ &= \Phi_k P_k \Phi_k^T + \Gamma_k R_{k/k+1} \Gamma_k^T \\ &\quad + \Phi_k E\{\tilde{X}_k \tilde{z}_{k/k+1}^T\} \Gamma_k^T + \Gamma_k E\{\tilde{z}_{k/k+1} \tilde{X}_k^T\} \Phi_k^T \end{aligned} \quad (31)$$

where $R_{k/k+1}$ denotes the covariance of the displacement estimates, a quantity which is computed by many displacement estimation algorithms. A common simplifying assumption in the literature (e.g., [2], [7]) is that the measurement noise, $\tilde{z}_{k/k+1}$, and state error, \tilde{X}_k , are uncorrelated, and thus the last two terms in (31) are set to zero. However, this assumption does *not generally hold when correlations exist between consecutive displacement estimates*. In particular, by linearizing the state propagation equation at t_k , we obtain (cf. (29)):

$$\begin{aligned} E\{\tilde{z}_{k/k+1} \tilde{X}_k^T\} &= E\left\{\tilde{z}_{k/k+1} \left(\Phi_{k-1} \tilde{X}_{k-1} + \Gamma_{k-1} \tilde{z}_{k-1/k}\right)^T\right\} \\ &= E\{\tilde{z}_{k/k+1} \tilde{X}_{k-1}^T\} \Phi_{k-1}^T + E\{\tilde{z}_{k/k+1} \tilde{z}_{k-1/k}^T\} \Gamma_{k-1}^T \\ &= E\{\tilde{z}_{k/k+1} \tilde{z}_{k-1/k}^T\} \Gamma_{k-1}^T. \end{aligned} \quad (32)$$

Note that the error term \tilde{X}_{k-1} depends on the measurement errors of all exteroceptive measurements up to and including time-step $k-1$, while the error term $\tilde{z}_{k/k+1}$ depends on the measurement errors at time-steps k and $k+1$ (cf. (2)). As a result, the errors \tilde{X}_{k-1} and $\tilde{z}_{k/k+1}$ are independent. Therefore, by applying the zero-mean assumption for the error $\tilde{z}_{k/k+1}$ we obtain $E\{\tilde{z}_{k/k+1} \tilde{X}_{k-1}^T\} = 0$. Employing the result of (4) and substituting from (32) in (31), we obtain the following expression for the propagation of the pose covariance in the case of inferred displacement measurements:

$$\begin{aligned} P_{k+1} &= \Phi_k P_k \Phi_k^T + \Gamma_k R_{k/k+1} \Gamma_k^T \\ &\quad + \Phi_k \Gamma_{k-1} J_{k-1/k}^k R_k J_{k/k+1}^{k T} \Gamma_k^T \\ &\quad + \Gamma_k J_{k/k+1}^k R_k J_{k-1/k}^{k T} \Gamma_{k-1}^T \Phi_k^T \end{aligned} \quad (33)$$

The experimental results presented in Section VII-B demonstrate that covariance estimates based on (33) more accurately represent the uncertainty in the robot's pose as compared to the case where the correlation terms in (31) are ignored.

V. EXTENSIONS

A. Treatment of Additional Measurements

In order to simplify the presentation in Section III, it was assumed that only proprioceptive and relative-pose measurements are available. However, this assumption is not necessary, as additional measurements can be processed in the standard EKF methodology [20]. For example, let

$$z_{k+\ell} = \zeta(X_{k+\ell}) + n_{k+\ell}$$

be an exteroceptive measurement received at time-step $k + \ell$. By linearizing, we obtain the measurement error equation:

$$\begin{aligned} \tilde{z}_{k+\ell} &= H'_{k+\ell} \tilde{X}_{k+\ell|k} + n \\ &= [0 \quad H'_{k+\ell} \quad 0] \begin{bmatrix} \tilde{X}_{k|k} \\ \tilde{X}_{k+\ell|k} \\ \tilde{z}_k \end{bmatrix} + n \end{aligned} \quad (34)$$

Since this expression adheres to the standard EKF model, the augmented filter state can be updated without any modifications to the algorithm. However, if additional measurements are processed, the compact expressions of (14) and (21) are no longer valid, as update steps occur between consecutive displacement estimates. In this case, (13) and (20) should be used during the propagation and update steps.

Another practically important case occurs when more than one sensor provides relative-pose measurements, but at different update rates. Such a situation would arise, for example, when a mobile robot is equipped with a camera and a laser range finder. In such a scenario, the state-augmentation approach of the SC-KF still applies. In particular, every time either of the sensors records a measurement, cloning is applied. Therefore, at any given time the filter state vector is comprised of i) three instances of the robot state, corresponding to the current state, and the state at the last time instants where each sensor received a measurement, and ii) the errors in the latest exteroceptive measurement of each sensor. Although the propagation and update equations must be modified to account for the change in dimension of the state vector, the basic principles of the approach still apply.

B. Extension to Multiple States

In the basic SC-KF algorithm presented in Section III, feature measurements are processed to construct *displacement estimates*, which subsequently define *constraints* between consecutive robot poses. By including two robot poses in the filter state vector, the SC-KF can optimally process successive exteroceptive measurements, while incurring a computational cost linear in the number of observed features. However, when a static feature is observed more than two times, the basic SC-KF must be modified. Intuitively, the observation of a static feature from multiple robot poses should impose a *geometric constraint* involving these measurements and all of the corresponding poses. We now briefly describe an extension to the basic SC-KF approach that correctly incorporates multiple observations of a single point feature while still maintaining computational complexity *linear* in the number of locally observed features.

Let Y_{f_j} be the position of a static feature, which is observed from $L \geq 2$ consecutive robot poses, $X_k, X_{k+1}, \dots, X_{k+L-1}$. The measurement function, h_{f_j} , corresponding to these measurements is

$$z_{k+i}^{f_j} = h_{f_j}(X_{k+i}, Y_{f_j}) + n_i^{f_j}, \quad \text{for } i = 0 \dots L-1 \quad (35)$$

where $n_i^{f_j}$ is the measurement noise. Stacking these L equations results in a block measurement equation of the form:

$$\mathbf{z}_{f_j} = \mathbf{h}_{f_j}(X_k, X_{k+1}, \dots, X_{k+L-1}, Y_{f_j}) + \mathbf{n}_{f_j}. \quad (36)$$

Eliminating the feature position, Y_{f_j} , from (36) yields a constraint vector that involves all of the robot poses:

$$\mathbf{c}_{f_j}(X_k, X_{k+1}, \dots, X_{k+L-1}, \mathbf{z}_{f_j}, \mathbf{n}_{f_j}) = \mathbf{0}_q \quad (37)$$

where q is the dimension of the constraint vector \mathbf{c}_{f_j} . If the EKF state vector has been augmented to include the L copies of the robot pose, the above equation can be used to perform an EKF update, thus utilizing all the geometric information provided by the observations of this feature. Furthermore, if M_k features are observed from L robot poses, then a constraint vector, \mathbf{c}_{f_j} , $j = 1 \dots M_k$, can be written for each of these features. Since the feature measurements are mutually uncorrelated, the resulting constraints will also be uncorrelated, and therefore, an EKF update that utilizes all M_k constraints can be performed in $O(M_k)$ time. The details of this extension are given in [21].

VI. RELATION TO SLAM

An alternative approach to processing the feature measurements obtained with an exteroceptive sensor is to jointly estimate the robot's pose and the feature positions. This is the well-known SLAM problem, which has been jwbe extensively studied (e.g., [22]–[25]). This section examines the relation of the SC-KF algorithm to SLAM.

1) *Computational complexity*: If an exact solution to SLAM was possible, the resulting pose estimates would be optimal, since all positioning information and all inter-dependencies between the robot and the features would be incorporated. However, good localization performance comes at a considerable computational cost. It is well known that the computational complexity and memory requirements of the EKF solution to SLAM increase quadratically with the number of features [22]. While several approximate solutions exist that possess lower computational complexity (e.g., [23], [25], [26]), many of them cannot guarantee the consistency of the estimates, nor is there a concrete measure of suboptimality.

Since the high computational burden of SLAM is due to the need to maintain a map of the environment, the amount of computational resources allocated for localization constantly increases as the robot navigates in an unknown environment. For continual operation over an extended period, this overhead can become unacceptably large. Even in an approximate SLAM algorithm, the largest portion of the computational resources is devoted to maintaining the constantly expanding feature map. However, there exist a number of applications where building a map is not necessary,

while real-time performance is of utmost importance (e.g., in autonomous aircraft landing [27], or emergency response). Such applications require high localization accuracy, but with minimal computational overhead.

Our proposed solution relies on employing *pairs* of consecutive exteroceptive measurements in order to produce displacement estimates, which are then fused with proprioceptive sensing information. As shown in Section III-F, our algorithm's complexity is linear in the number of features observed *only at each time-step*. In most cases this number is orders of magnitude smaller than the number of features in the environment. A reduced complexity SLAM approach that is similar in spirit to the SC-KF would consist of maintaining only the most recently acquired *local* features, i.e., those that are currently visible by the robot, in the state vector. However, the *algorithmic complexity* of such an EKF-SLAM would be *quadratic* in the number of local features. In contrast, the SC-KF is *linear* in the number of local features.

2) *Feature position observability:* SLAM algorithms also require the states of the local features to be completely observable, in order to be included in the state vector. When a single measurement does not provide sufficient information to initialize a feature's position estimate with bounded uncertainty, feature initialization schemes **must** be implemented [28], [29]. In fact, state augmentation is an integral part of many methods for delayed feature initialization [30], [31]. In contrast, in the SC-KF framework, feature initialization is not required since the *feature measurements* are included in the augmented state vector, instead of the *feature positions*.

3) *Data association:* Since **only pairs of exteroceptive measurements are used by the SC-KF algorithm**, the data association problem is simplified. Because SLAM requires a correspondence search over *all* map features in the robot's vicinity, its computational overhead is considerably higher [32]. To facilitate robust data association, it is common practice to employ a feature detection algorithm that extracts 'high-level' features (e.g., landmarks such as corners, junctions, straight-line segments) from raw sensor data. Then, *only* these features are employed for SLAM.

4) *Information loss:* While the extraction of high-level features results in more robust and computationally tractable algorithms (e.g., laser scans consist of hundreds of range points, but may contain only a few corner features), this approach, effectively *discards information* contained in the sensor data (cf. Fig. 1). The feature-based estimates of the robot's pose are suboptimal compared to those that use all the available information. Maintaining and processing the entire history of raw sensor input (e.g., [33]) can lead to excellent localization performance, but such an approach may be infeasible for real-time implementation on typical mobile robots. Conversely, the SC-KF approach typically takes advantage of the available information in two consecutive exteroceptive measurements (i.e., most laser points in two scans can be used to estimate displacement by scan matching).

5) *SC-KF and SLAM:* At this point, The SC-KF approach essentially offers an "enhanced" form of Dead Reckoning, and the robot's state uncertainty monotonically increases over time. For longer robot traverses the positioning accuracy obtained

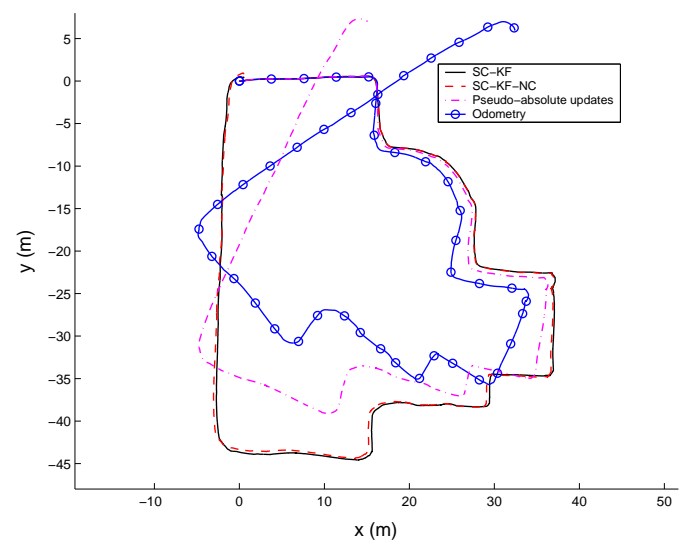


Fig. 2. The estimated trajectory of the robot using the SC-KF algorithm (solid line), the SC-KF-NC algorithm (dashed line), the method of [10] that uses absolute position pseudo-measurements (dash-dotted line), and odometry only (solid line with circles).

by this approach will be inferior to that of SLAM, as *no loop closing* occurs. The rate of uncertainty increase, though, is significantly lower than that attained when only proprioceptive measurements are used (cf. Section VII). However, as mentioned in Section III-F, in the SC-KF approach the state vector X_k is *not* required to contain only the robot's pose. If high-level, stable features (**landmarks**) are available, their positions can be included in the "robot" state vector X_k . Therefore, the SC-KF method for processing relative-state measurements can be expanded and integrated with the SLAM framework. This integration would further improve the attainable localization accuracy within areas with lengthy loops. Since this modification is beyond the scope of this work, in the following section we present experimental results applying the SC-KF methodology for the case where only relative-state and proprioceptive measurements are considered.

VII. EXPERIMENTAL RESULTS

I'm guessing that you used a Sick ladar.
please correct if necessary

This section presents experimental results that demonstrate the performance of the algorithms described in Sections III and IV. The experiments use a Pioneer II mobile robot equipped with a Sick LMS-200 laser rangefinder. The robot's pose consists of its planar position and orientation in a global frame:

$$X_k = [{}^G x_k \quad {}^G y_k \quad {}^G \phi_k]^T = [{}^G p_k^T \quad {}^G \phi_k]^T .(38)$$

We first present results from the application of the SC-KF, and then study the case where the robot's state is propagated based on displacement estimates exclusively (i.e., no proprioceptive measurements are available).

A. Stochastic Cloning Kalman Filter

In this experiment, odometry measurements are fused with displacement measurements that are obtained by laser scan matching with the method presented in [6]. The SC-KF equations for the particular odometry and measurement model employed in these experiments are presented in [34].

1) *Experiment description:* During the first experiment, the robot traversed a trajectory of approximately 165 m, while recording 378 laser scans. The robot processed a new laser scan approximately every 1.5 m, or every time its orientation changed by 10°. We here compare the performance of the SC-KF algorithm to that obtained b the approach of Hoffman *et al.* [10]. In [10], the displacement estimates and the previous pose estimates are combined to yield pseudo-measurements of the robot's absolute position. In order to guarantee consistent estimates for the latter case, we have employed the Covariance Intersection (CI) method [35] for fusing the pseudo-measurements of absolute position with the most current pose estimates. From here on we refer to this approach as "pseudo-absolute updates".

As discussed in Section III-F, the SC-KF has computational complexity linear in the number of feature measurements taken at each pose. If even this computational complexity is deemed too high for a particular application, one can ignore the correlations between consecutive displacement measurements, at the expense of optimality. In that case, the augmented state only contains the two copies of the robot state [9]. Results for this approximate, though computationally simpler, variant of the SC-KF, referred to as SC-KF-NC (i.e., no correlations between the measurement errors are considered) are present below and are compared with the performance of the SC-KF.

The robot trajectories estimated by the different algorithms are shown in Fig. 2. Fig. 3 presents the covariance estimates for the robot pose as a function of time. We observe that correctly accounting for the correlations between consecutive displacement estimates in the SC-KF, results in smaller covariance values. Even though ground truth for the entire trajectory is not known, the final robot pose is known to coincide with the initial one. The errors in the final robot pose are equal to $\tilde{X} = [0.5\text{m} \ 0.44\text{m} \ -0.11^\circ]^T$ (0.4% of the trajectory length) for the SC-KF, $\tilde{X} = [0.61\text{m} \ 0.65\text{m} \ -0.13^\circ]^T$ (0.54% of the trajectory length) for the SC-KF-NC, $\tilde{X} = [15.03\text{m} \ 7.07\text{m} \ -32.3^\circ]^T$ (10.6% of the trajectory length) for the approach of [10], and $\tilde{X} = [32.4\text{m} \ 5.95\text{m} \ -69.9^\circ]^T$ (19.9% of the trajectory length) for Dead Reckoning based on odometry. From these error values, as well as from visual inspection of the trajectory estimates in Fig. 2, we conclude that both the SC-KF and the SC-KF-NC yield very similar results. However, the approach based on creating pseudo-measurements of the absolute pose [10] performs significantly worse. It should be noted, that the errors in the final robot pose are consistent with the estimated covariance in all cases considered.

2) *Impact of correlations:* Clearly, the lack of ground truth data along the entire trajectory for the real-world experiment does not allow for a detailed comparison of the performance of the SC-KF and SC-KF-NC algorithms, as both appear to attain comparable estimation accuracy. Simulations are used

to perform a more thorough assessment of the impact of the measurement correlations on the position accuracy and the uncertainty estimates. The primary objective of these simulations is to contrast the behavior of the estimation errors with the computed covariance values in the cases when the correlations between consecutive measurements are accounted for (SC-KF), vs. when they are ignored (SC-KF-NC).

For the simulation results shown here, a robot moves in a circular trajectory of radius 4 m, while observing a wall that lies 6 m from the center of its trajectory. The relative-pose measurements in this case are created by performing line-matching, instead of point matching between consecutive scans [36]. Since only one line is available, the motion of the robot along the line direction is unobservable. As a result, the singular value decomposition of the covariance matrix of the robot's displacement estimate can be written as

$$R_{k/k+m} = [V_u \ V_o] \begin{bmatrix} s_1 & 0 & 0 \\ 0 & s_2 & 0 \\ 0 & 0 & s_3 \end{bmatrix} \begin{bmatrix} V_u^T \\ V_o^T \end{bmatrix}, \quad s_1 \rightarrow \infty$$

where V_u is the basis vector of the unobservable direction (i.e., a unit vector along the direction of the wall, expressed with respect to the robot frame at time step k) and V_o is a 3×2 matrix, whose column vectors form the basis of the observable subspace. To avoid numerical instability in the filter, the displacement measurements, $z_{k/k+m}$ computed by line-matching are projected onto the observable subspace, thus creating a relative-state measurement of dimension 2, given by $z'_{k/k+m} = V_o^T z_{k/k+m}$.

Fig. 4 shows the robot pose errors (solid lines), along with the corresponding 99.8th percentile of their distribution (dashed lines). The left column shows the results for the SC-KF algorithm presented in Section III, while the right one for the SC-KF-NC algorithm. As evident from Fig. 4, the covariance estimates of the SC-KF-NC are not commensurate with the corresponding errors. When the temporal correlations of the measurements are properly treated, as is the case for the SC-KF, substantially more accurate covariance estimates, that reflect the true uncertainty of the robot's state, are computed. Moreover, evaluation of the rms value of the pose errors shows that the errors associated with the SC-KF algorithm (which accounts for correlations) are 25% smaller than those of the SC-KF-NC.

B. State Propagation based on Displacement Estimates

We now present results for the case in which the robot's pose is estimated using only displacement estimates computed from laser scan matching. Given a displacement estimate $z_{k/k+m} = [{}^k \hat{p}_{k+m}^T \ {}^k \hat{\phi}_{k+m}]^T$, the global robot pose is propagated using the equations

$$\begin{aligned} \hat{X}_{k+m} &= g(X_k, z_{k/k+m}) \Rightarrow \\ \begin{bmatrix} {}^G \hat{p}_{k+m} \\ {}^G \hat{\phi}_{k+m} \end{bmatrix} &= \begin{bmatrix} {}^G \hat{p}_k \\ {}^G \hat{\phi}_k \end{bmatrix} + \begin{bmatrix} C({}^G \hat{\phi}_k) {}^k \hat{p}_{k+m} \\ {}^k \hat{\phi}_{k+m} \end{bmatrix} \end{aligned} \quad (39)$$

In this case, the Jacobian matrices Φ_k and Γ_k are given by

$$\Phi_k = \nabla_{\hat{X}_k} g = \begin{bmatrix} I & -\Psi C({}^G \hat{\phi}_k) {}^k \hat{p}_{k+m} \\ 0 & 1 \end{bmatrix}$$

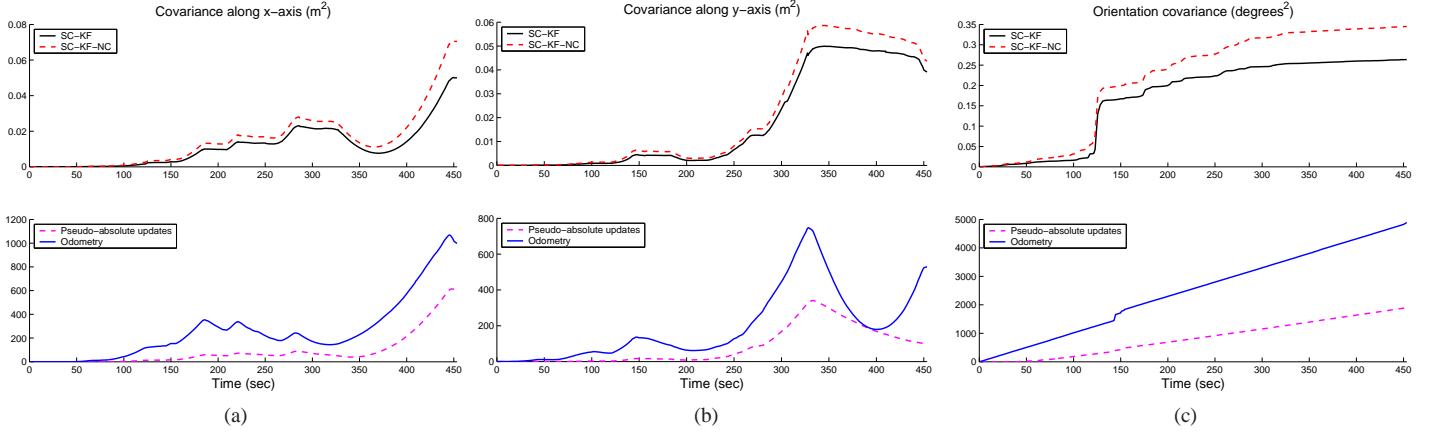


Fig. 3. The time evolution of the diagonal elements of the covariance matrix of the robot's pose. Note the difference in the vertical axes' scale. In these plots, the covariance values after filter updates are plotted.

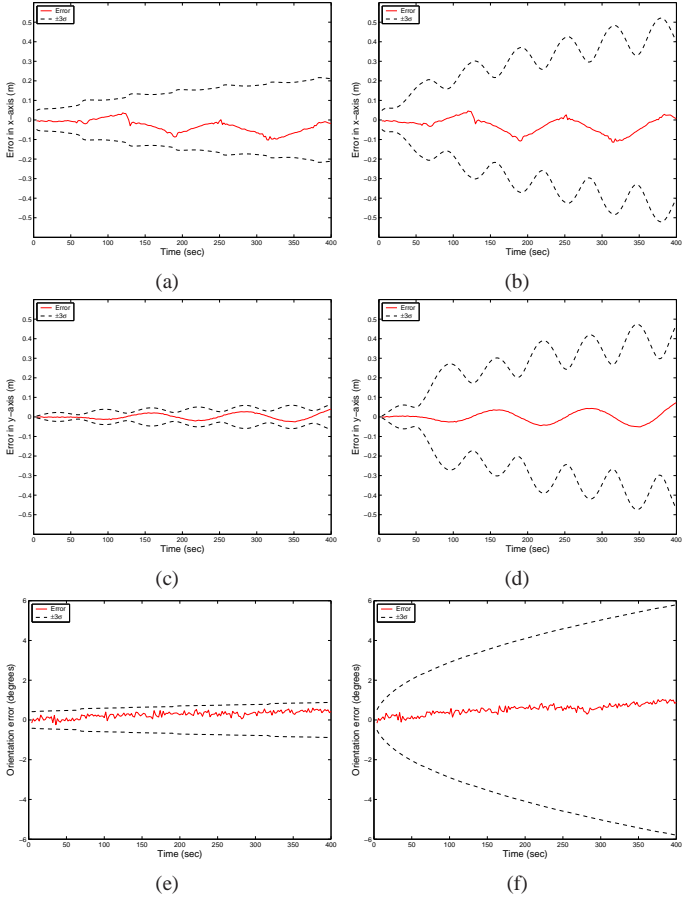


Fig. 4. The robot pose errors (solid lines) vs. the corresponding 99.8th percentile of their distribution, (dashed lines). The left column shows the results for the SC-KF algorithm proposed in this paper, while the right one demonstrates the results for the SC-KF-NC algorithm. In these plots, the covariance values after filter updates are plotted. (a - b) Errors and $\pm 3\sigma$ bounds along the x -axis (c - d) Errors and $\pm 3\sigma$ bounds along the y -axis (e - f) Orientation errors and $\pm 3\sigma$ bounds.

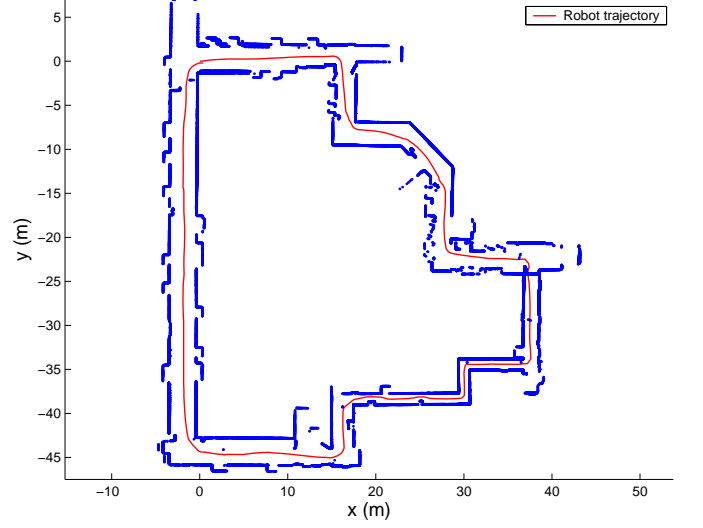


Fig. 5. The estimated trajectory of the robot based only on laser scan matching. The map is presented for visualization purposes only, by transforming all the laser points using the estimated robot pose. Some "spurious" points in the map are due to the presence of people.

$$\Gamma_k = \nabla_{\hat{z}_{k/k+m}} g = \begin{bmatrix} C(\hat{\phi}_k) & 0 \\ 0 & 1 \end{bmatrix}.$$

Fig. 5 presents the estimated robot trajectory, along with the map of the area that has been constructed by overlaying all the scan points, transformed using the estimates of the robot pose (we stress that the map is only plotted for visualization purposes, and is *not* estimated by the algorithm). This experiment used the same dataset from Section VII-A. Fig. 6 presents covariance estimates for the robot's pose, computed using (33) (SC-KF, solid lines) in contrast with those computed when the correlations between the consecutive displacement estimates are ignored (SC-KF-NC, dashed lines). As expected, the pose covariance is larger when only displacement measurements are used, compared to the case where odometry measurements are fused with displacement measurements (cf. Fig. 3). From Fig. 6 we observe that accounting for the correlations results in significantly *smaller* values for the covariance of the robot's pose estimates.

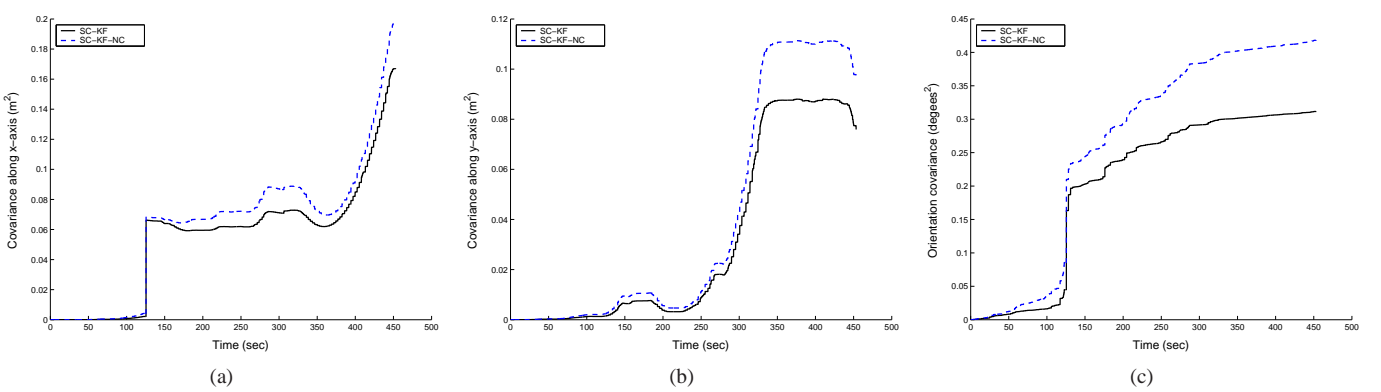


Fig. 6. The estimated covariance of the robot's pose when the correlation between consecutive measurements is properly accounted for (solid lines) vs. the covariance estimated when the correlations are ignored (dashed lines). (a) Covariance along the x -axis (b) Covariance along the y -axis (c) Orientation Covariance. At approximately 130 sec, a displacement estimate based on very few laser points was computed, resulting in a sudden increase in the covariance.

C. Investigation of the effects of correlations

Based on numerous experiments and simulation tests, the results of Fig. 6 (i.e., smaller covariance values when the correlations between displacement measurements are accounted for) are typical. We attribute this result to the fact that the correlation between consecutive relative-pose estimates tends to be negative. An intuitive explanation for this observation can be given by means of a simple example, for **1-dimensional motion**. Consider a robot moving on a straight line, and recording measurements, z_k , of the distance to a single feature on the same line. If at time-step k the error in the distance measurement is equal to $\epsilon_k > 0$, this error will contribute towards *underestimating* the robot's displacement during the interval $[k-1, k]$, but will contribute towards *overestimating* the displacement during the interval $[k, k+1]$. Therefore, the error ϵ_k has *opposite* effects on the two displacement estimates, rendering them negatively correlated.

In this 1D example, it is interesting to examine the time evolution of the covariance when the correlations are properly treated. Note that the robot's displacement can be computed as the difference of two consecutive distance measurements, i.e., $z_{k/k+1} = z_k - z_{k+1}$. If the covariance of the individual distance measurements is equal to $R_k = R_{k+1} = \sigma^2$, then the covariance of $z_{k/k+1}$ is equal to $R_{k/k+1} = 2\sigma^2$. Moreover, for this example it is easy to see that all the Jacobians in (33) are constant, and given by $J_{k/k+1}^k = 1$, $J_{k/k+1}^{k+1} = -1$, $\Phi_k = \Gamma_k = \Gamma_{k-1} = 1$. Substituting these values in (33), we obtain the following equation for covariance propagation in this case:

$$P_{k+1} = P_k + R_{k/k+1} - R_k - R_k = P_k. \quad (40)$$

We thus see that the covariance of the robot's position estimate remains *constant* during propagation when the correlations are properly treated. This occurs due because the error in the measurement z_k effectively "cancels out". On the other hand, if the correlations between consecutive displacement measurements are ignored, we obtain

$$P_{k+1} = P_k + R_{k/k+1} = P_k + 2\sigma^2. \quad (41)$$

In this case the position covariance increases linearly, a result that does not reflect the evolution of the true state uncertainty.

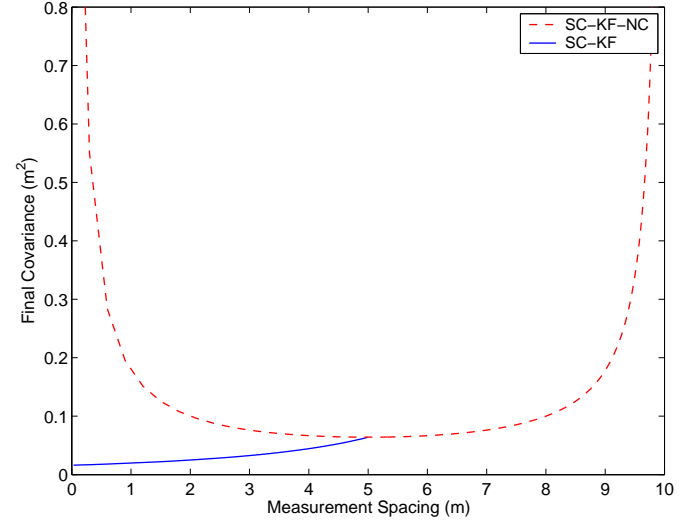


Fig. 7. The covariance estimates at the end of a 100 m trajectory using the expression of (33) (solid line), vs. when the correlations between consecutive displacement measurements are not accounted for (dashed line). Note that when the measurements occur more than 5 m apart, no correlations exist, and the two estimates are identical.

In the context of this 1D example, we next study the behavior of the covariance when features come in and out of the robot's Field Of View (FOV). Assume that a uniform distribution of features, with density ρ , exists on the line, and that the robot's FOV is limited to ℓ_{\max} . If the robot moves by $\Delta\ell$ between the time instants the measurements are recorded, then the overlap in the FOV at consecutive time instants is $\ell_{\max} - \Delta\ell$. Within this region lie $M_k = \rho(\ell_{\max} - \Delta\ell)$ features, whose measurements are used for displacement estimation. The least-squares displacement estimate is given by:

$$z_{k/k+1} = \frac{1}{M_k} \sum_{i=1}^{M_k} (z_{k_i} - z_{k+1_i}) \quad (42)$$

where z_{k_i} and z_{k+1_i} are the measurements to the i -th feature at time-steps k and $k+1$, respectively. The covariance of $z_{k/k+1}$ is given by:

$$R_{k/k+1} = \frac{2\sigma^2}{M_k} = \frac{2\sigma^2}{\rho(\ell_{\max} - \Delta\ell)}. \quad (43)$$

Thus, if one ignores the correlations between consecutive displacement estimates, the covariance propagation equation is:

$$P_{k+1} = P_k + \frac{2\sigma^2}{\rho(\ell_{\max} - \Delta\ell)} . \quad (44)$$

At the end of a path of length ℓ_{total} (i.e., after $\ell_{\text{total}}/\Delta\ell$ propagation steps), the estimated covariance of the robot position, starting from a zero initial value, will be given by:

$$P_{\text{final}} = \frac{\ell_{\text{total}}}{\Delta\ell} \frac{2\sigma^2}{\rho(\ell_{\max} - \Delta\ell)} . \quad (45)$$

We now derive the corresponding covariance equations for the case that the correlations are properly incorporated. Since the robot moves by a distance $\Delta\ell$ between the time instants when the measurements are recorded, the number of features that are observed at three consecutive time instants (i.e., $k-1$, k , and $k+1$), is $\rho(\ell_{\max} - 2\Delta\ell)$. Employing this observation to evaluate the Jacobians in (33) yields the following expression for the propagation of the covariance:

$$P_{k+1} = P_k + \frac{2\sigma^2 \Delta\ell}{\rho(\ell_{\max} - \Delta\ell)^2}, \quad \text{for } \ell_{\max} > 2\Delta\ell . \quad (46)$$

Note that if $\ell_{\max} < 2\Delta\ell$, no overlap exists between the FOV at time instants $k-1$ and $k+1$, and thus no feature measurement can be used for computing two displacement estimates. In that case, expression (44) is exact. At the end of a path of length ℓ_{total} , the covariance of the robot position is:

$$P_{\text{final}} = \frac{2\sigma^2 \ell_{\text{total}}}{\rho(\ell_{\max} - \Delta\ell)^2}, \quad \text{for } \ell_{\max} > 2\Delta\ell . \quad (47)$$

Fig. 7 plots the variance in the robot's position at the end of a trajectory of length $\ell_{\text{total}} = 100$ m, as a function of the size of the robot's displacement between consecutive measurements. The solid line corresponds to the case when the correlations between displacement measurements are accounted for (cf. (47)), while the dashed line corresponds to the case when these are ignored (cf. (45)). The parameters used to generate this plot are: the feature density is $\rho = 5$ features/m, the robot's FOV is $\ell_{\max} = 10$ m, and the standard deviation of each distance measurement is $\sigma = 0.2$ m. It is important to note that when the correlations between consecutive measurements are accounted for, the final uncertainty is a monotonically increasing function of the displacement between measurements, $\Delta\ell$. This agrees with intuition, which dictates that when measurements occur less frequently, the accuracy of the state estimates deteriorates. However, when the correlations between displacement measurements are ignored, the covariance estimates do not have this property. Fig. 7 shows that for $\Delta\ell < 5$ m, as measurements are recorded more frequently, the covariance estimates become larger. This behavior is clearly incorrect, and arises due to fact that the dependency between consecutive displacement estimates is ignored.

The preceding analysis substantiates, at least in the simple case of a robot moving in 1D, that the use of expression (33) for covariance propagation results in substantially more accurate covariance estimates. Unfortunately, for robots moving in 2D [4] and 3D [2], the covariance propagation equations are

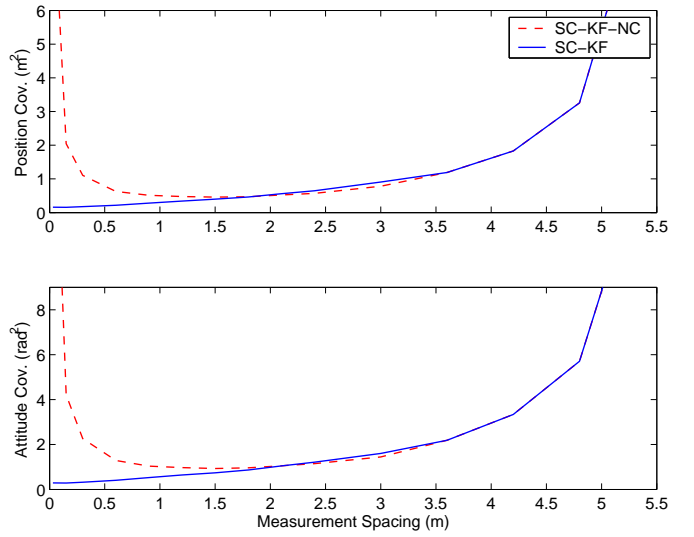


Fig. 8. The covariance estimates at the end of a 100 m trajectory, for a robot performing visual odometry with a stereo pair. The top plot shows the position uncertainty, while the bottom one the attitude uncertainty. When correlations are properly treated (solid lines), the covariance is a monotonic function of the measurement spacing. This is not the case when correlations are ignored (dashed lines).

time-varying. As a result, an analogous closed form analysis for general trajectories and arbitrary feature placement appears to be intractable. However, simulation experiments indicate that the conclusions drawn for the 1D case also apply to the more practical scenarios of robots moving in 2D and 3D. For example, Fig. 8 shows the position and attitude covariance at the end of a 100 m trajectory for a robot performing visual odometry with a stereo pair of cameras [2]. The plotted lines represent the traces of the submatrices of the covariance matrix corresponding respectively to position (top subplot) and attitude (bottom subplot). These plots once again show that the covariance is a monotonically increasing function of measurement spacing when the exact expression of (33) is employed, while an artificial ‘‘valley’’ appears when the correlation terms in (33) are ignored.

VIII. CONCLUSIONS

In this paper, we have proposed an efficient EKF-based estimation algorithm, termed a *Stochastic Cloning-Kalman Filtering* (SC-KF), for the problem of fusing proprioceptive measurements with relative-state measurements that are inferred from exteroceptive sensory input. An analysis of the structure of the measurement equations demonstrated that when the same exteroceptive measurements are processed to estimate displacement in consecutive time intervals, the displacement errors are temporally correlated. The main contribution of this work is the introduction of a novel feature-marginalization process that allows for the processing of relative-pose measurements while also considering the correlations between these. This method is based on augmenting the state vector of the EKF to temporarily include the robot poses and the feature observations related through a local geometric constraint (i.e., a relative-state measurement). By employing state augmentation, the dependence of the relative-state measurement on previous states and measurements is

transformed to a dependence on the *current* state of the filter, and this enables application of the standard EKF framework.

The experimental and simulation results demonstrate that the SC-KF method attains better localization performance compared to previous approaches [10], while the overhead imposed by the additional complexity is minimal. The method yields more accurate estimates, and most significantly, it provides a more precise description of the uncertainty in the robot's state estimates. Additionally, the method is versatile, since it is independent of the actual sensing modalities used to obtain the proprioceptive and exteroceptive measurements.

REFERENCES

- [1] A. Kelly, "General solution for linearized systematic error propagation in vehicle odometry," in *Proc. IEEE/RSJ Int. Conf. on Robots and Systems*, Maui, HI, Oct.29-Nov.3 2001, pp. 1938–45.
- [2] L. Matthies, "Dynamic stereo vision," Ph.D. dissertation, Dept. of Computer Science, Carnegie Mellon University, 1989.
- [3] C. Olson, L. Matthies, H. Schoppers, and M. Maimone, "Robust stereo ego-motion for long distance navigation," in *Proceedings of CVPR*, 2000, pp. 453–458.
- [4] F. Lu and E. Milios, "Robot pose estimation in unknown environments by matching 2d range scans," *Journal of Intelligent and Robotic Systems: Theory and Applications*, vol. 18, no. 3, pp. 249–275, Mar. 1997.
- [5] D. Silver, D. M. Bradley, and S. Thayer, "Scan matching for flooded subterranean voids," in *Proc. IEEE Conf. on Robotics, Automation and Mechatronics (RAM)*, Dec. 2004.
- [6] S. T. Pfister, K. L. Kriechbaum, S. I. Roumeliotis, and J. W. Burdick, "Weighted range sensor matching algorithms for mobile robot displacement estimation," in *Proc. IEEE Int. Conf. on Robotics and Automation*, Washington D.C., May 11-15 2002, pp. 1667–74.
- [7] K. Konolige, "Large-scale map-making," in *AAAI National Conference on Artificial Intelligence*, San Jose, CA, July 2004, pp. 457–463.
- [8] P. Torr and D. Murray, "The development and comparison of robust methods for estimating the fundamental matrix," *International Journal of Computer Vision*, vol. 24, no. 3, pp. 271–300, 1997.
- [9] S. I. Roumeliotis and J. W. Burdick, "Stochastic cloning: A generalized framework for processing relative state measurements," in *Proc. IEEE Int. Conf. on Robotics and Automation*, Washington D.C., 2002, pp. 1788–1795.
- [10] B. D. Hoffman, E. T. Baumgartner, T. L. Huntsberger, and P. S. Schenker, "Improved state estimation in challenging terrain," *Autonomous Robots*, vol. 6, no. 2, pp. 113–130, April 1999.
- [11] P. S. Maybeck, *Stochastic Models, Estimation, and Control*, ser. Mathematics in Science and Engineering. Academic Press, 1979, vol. 141-2.
- [12] A. I. Mourikis and S. I. Roumeliotis, "On the treatment of relative-pose measurements for mobile robot localization," in *Proc. IEEE Int. Conf. on Robotics and Automation*, Orlando, FL, May 15-19 2006, (to appear).
- [13] S. I. Roumeliotis, "A kalman filter for processing 3-d relative pose measurements," California Institute of Technology, Tech. Rep., Mar. 2002, http://robotics.caltech.edu/~stergios/tech_reports/relative_3d_kf.pdf.
- [14] S. Fleischer, "Bounded-error vision-based navigation of autonomous underwater vehicles," Ph.D. dissertation, Stanford University, 2000.
- [15] R. Eustice, H. Singh, and J. Leonard, "Exactly sparse delayed-state filters," in *Proc. IEEE Int. Conf. on Robotics and Automation*, Barcelona, Spain, April 2005, pp. 2428–2435.
- [16] R. Eustice, O. Pizarro, and H. Singh, "Visually augmented navigation in an unstructured environment using a delayed state history," in *Proc. IEEE Int. Conf. on Robotics and Automation*, New Orleans, LA, April 2004, pp. 25–32.
- [17] R. Garcia, J. Puig, O. Ridao, and X. Cufí, "Augmented state Kalman filtering for auv navigation," in *Proc. IEEE Int. Conf. on Robotics and Automation*, Washington, DC, May 2002, pp. 4010–4015.
- [18] F. Lu and E. Milios, "Globally consistent range scan alignment for environment mapping," *Autonomous Robots*, vol. 4, no. 4, 1997.
- [19] E. J. Lefferts, F. L. Markley, and M. D. Shuster, "Kalman filtering for spacecraft attitude estimation," *Journal of Guidance, Control, and Dynamics*, vol. 5, no. 5, pp. 417–429, Sept.-Oct. 1982.
- [20] D. Bayard and P. B. Brugarolas, "An estimation algorithm for vision-based exploration of small bodies in space," in *Proceedings of the 2005 American Control Conference*, Portland, OR, June 2005, pp. 4589–4595.
- [21] A. I. Mourikis and S. I. Roumeliotis, "A multi-state constraint Kalman filter for vision-aided inertial navigation," in *Proc. IEEE Int. Conf. on Robotics and Automation*, Rome, Italy, 2007, (submitted).
- [22] R. C. Smith, M. Self, and P. Cheeseman, *Autonomous Robot Vehicles*. Springer-Verlag, 1990, ch. Estimating Uncertain Spatial Relationships in Robotics, pp. 167–193.
- [23] M. Montemerlo, "FastSLAM: A factored solution to the simultaneous localization and mapping problem with unknown data association," Ph.D. dissertation, Robotics Institute, Carnegie Mellon University, July 2003.
- [24] S. Thrun, D. Koller, Z. Ghahramani, and H. Durrant-Whyte, "Simultaneous mapping and localization with sparse extended information filters: Theory and initial results," School of Computer Science, Carnegie Mellon University, Tech. Rep., 2002.
- [25] P. Newman, J. Leonard, J. D. Tardos, and J. Neira, "Explore and return: experimental validation of real-time concurrent mapping and localization," in *Proc. IEEE Int. Conf. on Robotics and Automation*, Washington, DC, May 11-15 2002, pp. 1802–9.
- [26] S. J. Julier and J. K. Uhlmann, "Simultaneous localisation and map building using split covariance intersection," in *Proc. IEEE/RSJ Int. Conf. on Intelligent Robots and Systems*, Maui, HI, Oct. 29-Nov. 3 2001, pp. 1257–62.
- [27] S. Roumeliotis, A. Johnson, and J. Montgomery, "Augmenting inertial navigation with image-based motion estimation," in *IEEE International Conference on Robotics and Automation*, Washington D.C., 2002, pp. 4326–33.
- [28] T. Bailey, "Constrained initialisation for bearing-only SLAM," in *Proc. IEEE Int. Conf. on Robotics and Automation*, vol. 2, Sept. 2003, pp. 1966–1971.
- [29] N. Kwok and G. Dissanayake, "An efficient multiple hypothesis filter for bearing-only SLAM," in *Proc. IEEE/RSJ Int. Conf. on Intelligent Robots and Systems*, vol. 1, Oct. 2004, pp. 736–741.
- [30] J. Leonard, R. Rikoski, P. Newman, and M. Bosse, "Mapping partially observable features from multiple uncertain vantage points," *Int. J. Robotics Research*, vol. 21, no. 10-11, pp. 943–975, 2002.
- [31] J. Leonard and R. Rikoski, "Incorporation of delayed decision making into stochastic mapping," *Experimental Robotics VII*, vol. 271, pp. 533–542, 2001.
- [32] J. Neira and J. D. Tardos, "Data association in stochastic mapping using the joint compatibility test," *IEEE Transactions on Robotics and Automation*, vol. 17, no. 6, pp. 890–897, 2001.
- [33] A. Howard, "Multi-robot mapping using manifold representations," in *Proc. 2004 IEEE Int Conf. on Robotics and Automation*, New Orleans, LA, April 2004, pp. 4198–4203.
- [34] A. I. Mourikis and S. I. Roumeliotis, "SC-KF mobile robot localization: A stochastic cloning-kalman filter for processing relative-state measurements," University of Minnesota, Dept. of Computer Science and Engineering, Tech. Rep., October 2006.
- [35] S. Julier and J. Uhlman, "A non-divergent estimation algorithm in the presence of unknown correlations," in *Proceedings of the American Control Conference*, vol. 4, 1997, pp. 2369 – 2373.
- [36] S. T. Pfister, S. I. Roumeliotis, and J. W. Burdick, "Weighted line fitting algorithms for mobile robot map building and efficient data representation," in *Proc. IEEE Int. Conf. on Robotics and Automation*, Taipei, Taiwan, Sep. 14-19 2003, pp. 1304–1311.